Catalytic Mechanism of the Quinoenzyme Amine Oxidase from *Escherichia coli*: Exploring the Reductive Half-Reaction[†,‡]

Carrie M. Wilmot,[§] Jeremy M. Murray,[§] Gordon Alton,[||,⊥] Mark R. Parsons,[§] Maire A. Convery,[§] Veronica Blakeley,[§] Adam S. Corner,[§,▽] Monica M. Palcic,[||] Peter F. Knowles,[§] Michael J. McPherson,[§] and Simon E. V. Phillips*[,§]

Department of Biochemistry and Molecular Biology, University of Leeds, Leeds LS2 9JT, United Kingdom, and Department of Chemistry, University of Alberta, Edmonton, Alberta T6G 2G2, Canada

Received August 28, 1996; Revised Manuscript Received December 9, 1996[⊗]

ABSTRACT: The crystal structure of the complex between the copper amine oxidase from *Escherichia coli* (ECAO) and a covalently bound inhibitor, 2-hydrazinopyridine, has been determined to a resolution of 2.0 Å. The inhibitor covalently binds at the 5 position of the quinone ring of the cofactor, 2,4,5-trihydroxyphenylalaninequinone (TPQ). The inhibitor complex is analogous to the substrate Schiff base formed during the reaction with natural monoamine substrate. A proton is abstracted from a methylene group adjacent to the amine group by a catalytic base during the reaction. The inhibitor, however, has a nitrogen at this position, preventing proton abstraction and trapping the enzyme in a covalent complex. The electron density shows this nitrogen is hydrogen bonded to the side chain of Asp383, a totally conserved residue, identifying it as the probable catalytic base. The positioning of Asp383 is such that the *pro-S* proton of a substrate would be abstracted, consistent with the stereospecificity of the enzyme determined by ^{1}H NMR spectroscopy. Site-directed mutagenesis and *in vivo* suppression have been used to substitute Asp383 for 12 other residues. The resulting proteins either lack or, in the case of glutamic acid, have very low enzyme activity consistent with an essential catalytic role for Asp383. The O4 position on the quinone ring is involved in a short hydrogen bond with the hydroxyl of conserved residue Tyr369. The distance between the oxygens is less than 2.5 Å, consistent with a shared proton, and suggesting ionization at the O4 position of the quinone ring. The Tyr369 residue appears to play an important role in stabilizing the position of the quinone/inhibitor complex. The O2 position on the quinone ring is hydrogen bonded to the apical water ligand of the copper. The basal water ligand, which lies 2.0 Å from the copper in the native structure, is at a distance of 3.0 Å in the complex. In the native structure, the active site is completely buried, with no obvious route for entry of substrate. In the complex, the tip of the pyridine ring of the bound inhibitor is on the surface of the protein at the edge of the interface between domains 3 and 4, suggesting this as the entry point for the amine substrate.

Amine oxidases can be classified on the basis of cofactor, as either flavin (Berry *et al*., 1994) (EC 1.4.3.4)- or copper-containing (McIntire & Hartmann, 1993; Knowles & Dooley, 1994; Klinman & Mu, 1994) (EC 1.4.3.6). The copper-containing monoamine oxidases are ubiquitous, occurring in both prokaryotes and eukaryotes. The enzymes in prokaryotes, such as *Escherichia coli*, allow the organism to utilize various amine substrates as sources of carbon and nitrogen. In higher eukaryotes, their biological functions are less well defined, with roles suggested in detoxification and cell signalling in animals and cell wall cross-linking, lignification, and defense in plants.

The copper amine oxidases have been the subject of biochemical, spectroscopic, and kinetic study for many years (Klinman & Mu, 1994). The proteins are homodimers of 70−95 kDa monomers depending on their source. Each monomer contains a copper and an organic cofactor, 2,4,5-trihydroxyphenylalaninequinone (TPQ; Figure 1a), post-translationally derived from a tyrosine residue (Mu *et al*., 1992; Janes *et al*., 1992; Cooper *et al*., 1992). The formation of the quinone has been shown to be a self-processing event requiring both copper and molecular oxygen (Tanizawa, 1995).

Copper amine oxidases catalyze the oxidation of various primary amine substrates to their corresponding aldehydes, with the subsequent release of ammonia and hydrogen peroxide. Substrate preference depends on the enzyme source. *E. coli* monoamine oxidase (ECAO) preferentially catalyzes the oxidation of primary aromatic amines (Roh *et al*., 1994a). The proposed mechanism can be represented by a reductive half-reaction, leading to reduced enzyme and product aldehyde, and an oxidative half-reaction in which

[†] This work was supported by grants from the U.K. Biotechnology and Biological Sciences Research Council (BBSRC) and the Engineering and Physical Sciences Research Council to P.F.K. S.E.V.P., and M.J.M., from the Natural Sciences and Engineering Research Council of Canada, and from the Alberta Heritage Foundation for Medical Research (Canada) to M.M.P. J.M.M. is supported by a BBSRC Special Studentship. S.E.V.P. is an International Research Scholar of the Howard Hughes Medical Institute.

[‡] File name for the Brookhaven Protein Structure Data Bank entry is 1SPU. Structure factors for Brookhaven Protein Structure Data Bank entry R1SPUSF.

* Author to whom correspondence should be addressed.

[§] University of Leeds.

[||] University of Alberta.

[⊥] Present address: The Burnham Institute, 10901 N. Torrey Pines Rd., La Jolla, CA 92037.

[▽] Present address: Department of Immunology, Babraham Institute, Babraham, Cambridge CB2 4AT, United Kingdom.

[⊗] Abstract published in *Advance ACS Abstracts,* February 1, 1997.

S0006-2960(96)02205-2 CCC: $14.00

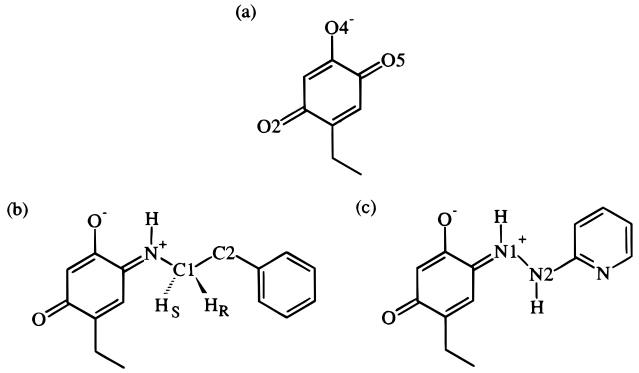

FIGURE 1: Chemical forms of the TPQ cofactor in *E. coli* monoamine oxidase. Labeling of atoms corresponds to the text, except for H_S and H_R which correspond to the *pro-S* and *pro-R* protons, respectively. (a) The form of TPQ found in the resting state of the active enzyme. (b) The substrate Schiff base intermediate of the reductive half-cycle, with phenylethylamine as substrate. (c) The covalent inhibitor complex between 2-HP and TPQ. This mimics the substrate Schiff base intermediate.

molecular oxygen is required to reoxidize the enzyme, with production of ammonia and hydrogen peroxide (Klinman & Mu, 1994). During the reductive half-reaction, a Schiff base complex is formed between the substrate and TPQ (Figure 1b). Evidence for this intermediate comes from reductive trapping experiments (Hartmann & Klinman, 1987, 1990). On the basis of spectroscopic comparison with model compounds, the substrate is thought to bind at the 5 position of the quinone ring (Brown *et al*., 1991; Mure & Klinman, 1993). Proton abstraction from the C1 position of the substrate leads to the formation of the product aldehyde and a reduced aminoquinol form of the enzyme (Janes & Klinman, 1991). Intriguingly, the stereochemistry of the proton abstraction varies depending on the enzyme source (Coleman *et al*., 1991; Scaman & Palcic, 1992). Enzymes isolated from pea seedling, soybean seedling, chick pea seedling, and pig kidney have been shown to be *pro-S* specific for C1 hydrogen abstraction from tyramine (Coleman *et al*., 1989, 1991). The copper amine oxidases from pig and horse plasma are *pro-R* specific for C1 of tyramine or dopamine (Coleman *et al*., 1991; Palcic *et al*., 1995). Amine oxidases that catalyze net nonstereospecific C1 hydrogen abstraction have been characterized from the plasma of cow, sheep, and rabbit (Farnum & Klinman, 1986; Coleman *et al*., 1991). In contrast to tyramine C1 stereochemistry, the oxidative deamination of benzylamine occurs with stereospecific removal of the *pro-S* hydrogen for all enzymes studied (Battersby *et al*., 1976, 1979; Alton *et al*., 1995; Palcic *et al*., 1995). A reversible imine−enamine tautomerization preceding imine hydrolysis has been demonstrated in many amine oxidases and allows exchange of C2 hydrogens from tyramine or dopamine with bulk solvent (Figure 2; Lovenberg & Beaven, 1971). Furthermore, the stereochemistry of C1 hydrogen abstraction from tyramine or dopamine is correlated with the hydrogen exchange reactions at C2 of these substrates (Farnum & Klinman, 1986; Palcic *et al*., 1995). The soluble *pro-S* specific copper amine oxidases do not catalyze hydrogen exchange at C2, whereas *pro-R* and net nonstereospecific enzymes do catalyze C2 exchange (Lovenberg & Beaven, 1971; Coleman *et al*., 1991). The group acting as the proton-abstracting base in the enzyme has been tentatively identified as a carboxylate group on the basis of a pK_a of ~5, derived from pH-dependent studies on bovine serum amine oxidase (Farnum *et al*., 1986).

Recently, the structure of *E. coli* amine oxidase (ECAO) has been solved by X-ray crystallography (Parsons *et al*., 1995). Each monomer consists of 727 amino acids (Azakami *et al*., 1994) and four structural domains. The dimer resembles a mushroom. The largest domain, D4, located at the C terminus, consists of a 440-residue β-sandwich, which contains the active site and forms the bulk of the dimer interface. The N-terminal α/β-domain (D1) that forms the stalk of the mushroom consists of 85 residues and is not present in all amine oxidases. The two remaining α/β-domains, D2 and D3, are situated at the outer edge of the mushroom cap. They are each composed of around 100 amino acids and are homologous to one another in both structure and amino acid sequence. Two pairs of β-hairpin arms of the D4 β-sandwich are elongated and reach across from one monomer to the other. One pair links the two active sites, while the other arm lies on the top of the D4 cap toward the peripheral D3. The overall structure of the dimer is shown in Figure 3. In a crystal form shown to contain catalytically active protein, and whose structure was solved to 2.4 Å, the copper is coordinated by four basal ligands (His524, His526, His689, and a water) and a more weakly bound apical water in a distorted square pyramidal configuration (Parsons *et al*., 1995). The TPQ itself is not a ligand to the copper but lies nearby. The overall position of the TPQ is clear, but the exact orientation and conformation of the ring are not. Due to the disorder in the ring orientation, it is not obvious how the substrate will bind in the active site. The TPQ lies close to several conserved residues: Asn465, Tyr369, and the candidate base, Asp383. The active site is also completely buried, with no obvious route for the entry of substrate.

Inhibitors of the copper monoamine oxidases are well known. ECAO has been shown to be completely and irreversibly inactivated by derivatives of hydrazine, such as phenelzine, isoniazid, tranycypromine (Roh *et al*., 1994a), and 2-hydrazinopyridine (2-HP) (Collison *et al*., 1989). These form a mimic of the Schiff base complexes between substrate and enzyme. In these inhibitors, the C1 position of the substrate is replaced by a nitrogen, and completion of the reaction to release product is prevented. The inhibited enzyme is therefore a covalent complex between the hydrazine-derived inhibitor and TPQ.

Here we present the crystal structure of the covalently linked complex between the inhibitor 2-hydrazinopyridine and *E. coli* amine oxidase, which reveals the identity of the catalytic base and indicates the mode of substrate binding. We also report the preliminary results of mutagenesis studies at Asp383, designed to test the potential role of this residue as the catalytic base, and the determination of the stereospecificity of the *E. coli* enzyme by ^{1}H NMR spectroscopy. The results provide new insight into substrate binding and catalytic events during the reductive half-reaction and are discussed in the context of our current mechanistic understanding of this class of enzyme.

MATERIALS AND METHODS

Protein Purification and Enzyme Assay. Enzyme for crystallization, activity *vs* pH studies, and stereochemistry experiments was prepared as previously reported (Parsons *et al*., 1995). Enzyme activity was assayed in two ways,

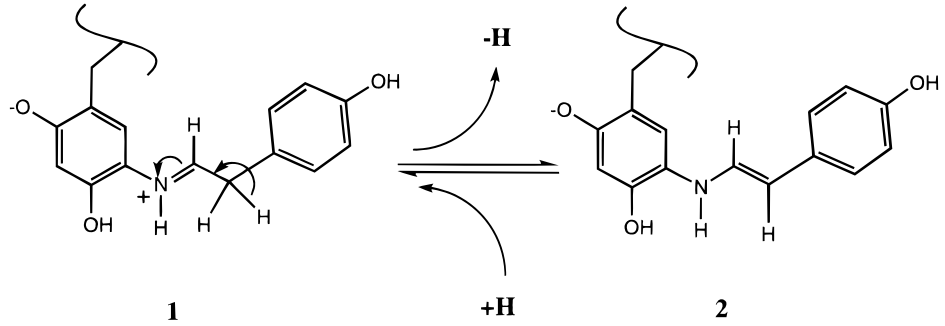

FIGURE 2: Reversible tautomerization of the putative tyramine/TPQ prehydrolysis intermediate. Loss of hydrogen from the product imine intermediate (**1**) yields the enamine (**2**). Reprotonation of enamine may occur from bulk solvent.

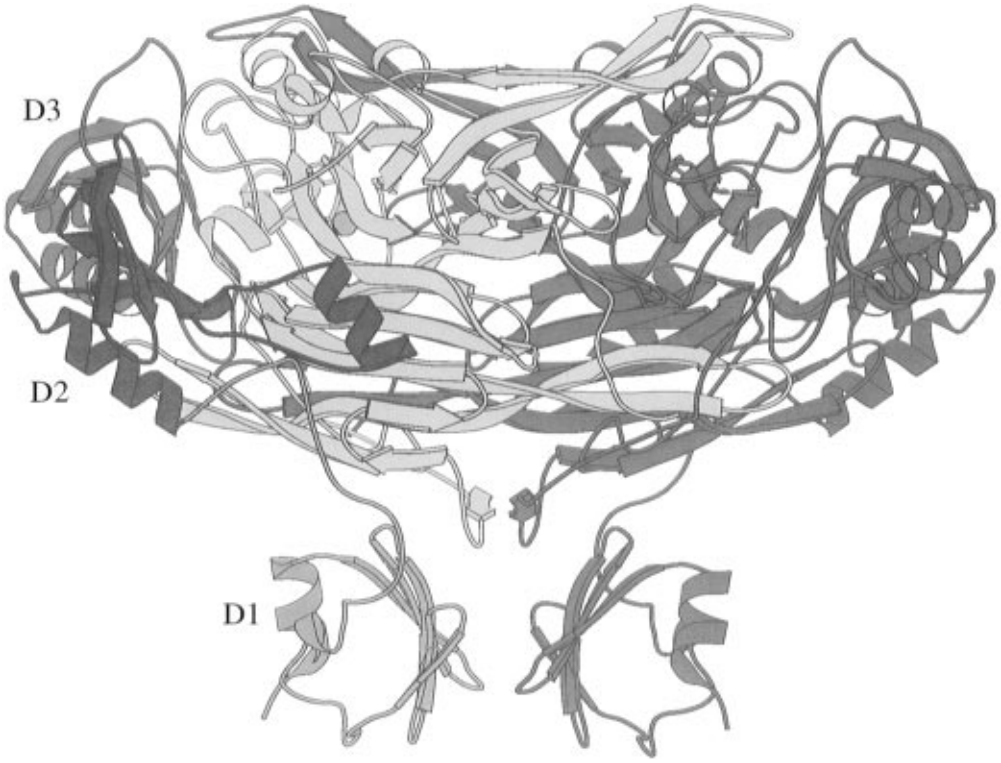

FIGURE 3: Ribbon representation of the fold of *E. coli* monoamine oxidase. Subunit A is colored by domains, numbered from the N terminus. The color scheme is as follows. Domain 1 (D1) is gray. Domain 2 (D2) is purple. Domain 3 (D3) is pink. Domain 4 is cyan. Subunit B is shown as a single color, red. The positions of the two coppers are shown as green spheres [figure generated using MOLSCRIPT (Kraulis, 1991)].

either using the coupled assay described in Parsons *et al*. (1995) or by the direct assay method of Parrott *et al*. (1987). Protein concentrations were estimated by the Bradford method using a Bio-Rad kit with bovine serum albumin as a standard (Bradford, 1976) for the stereochemistry experiments or by monitoring absorbance at 280 nm.

X-ray Crystallographic Data Collection. The catalytically competent native crystals were grown from sodium citrate and belong to the space group $P2_12_12_1$ with cell dimensions of $a = 135.6$ Å, $b = 167.8$ Å, and $c = 81.5$ Å (Roh *et al*., 1994b). The crystals were left soaking in 2-hydrazinopyridine (2-HP) dihydrochloride (Aldrich) solution made with crystal-stabilizing solution (1.4 M sodium citrate solution and 0.1 M HEPES buffer at pH 7.2). The crystals changed color from pink to orange. Two data sets were collected at Daresbury SRS (Synchrotron Radiation Source) station 9.6 on a 300 mm Mar imaging plate. Data collection statistics and soaking conditions are summarized in Table 1. To maximize reaction between 2-HP and TPQ, the second data set was collected from a crystal soaked in a 5-fold higher ratio of inhibitor to enzyme subunit, and for 30 times longer, than crystals used for the first data set. The crystal used in the second data set was flash-frozen to 100 K in a cold nitrogen stream (Oxford Cryosystems) during data collection. The cryoprotectant solution used was 20% glycerol in 1.44 M sodium citrate buffer at pH 6.4. The freezing process led to imperfect isomorphism with the initial data set collected at 277 K. The new cell dimensions were $a = 134.5$ Å, $b = 166.1$ Å, and $c = 79.4$ Å, a 2.6% decrease in the *c*-axis unit cell edge. The diffraction pattern was anisotropic upon freezing, with diffraction in the *c*-axis direction being more limited in resolution than in the *a*- and *b*-axes directions. Integration of the reflections was carried out using MOSFLM (Leslie, 1992). Data reduction was achieved using ROTAVATA and AGROVATA in the CCP4 suite of programs (Collaborative Computational Project Number 4, 1994).

X-ray Crystallographic Structure Solution. $2F_o - F_c$ and $F_{o(complex)} - F_{o(native)}$ (for the 277 K data set only) and $F_o - F_c$ difference maps were studied on an Evans and Sutherland

Table 1: Data Collection Statistics[a]

crystal	ratio of 2-HP:ECAO subunit/soak time	d_{min} (Å)	number of measurements	multiplicity	completeness (%)	number of crystals/data collection temperature	R_{symm}[b] (%)
active	1:1/1 day	2.5	162 939	2.8	91.3	8/277 K	6.3[c]
ECAO			(10 408)	(2.5)	(89.8)		(20.7)
active	5:1/30	2.0	264 608	2.6	83.7	1/100 K	5.7[d]
ECAO	days		(12 938)	(2.0)	(72.9)		(22.0)

[a] 2-HP = 2-hydrazinopyridine; ECAO = *E. coli* monoamine oxidase. [b] $R_{symm} = \sum_h|I(h)-\langle I(h)\rangle|/\sum_h|I(h)|$. [c] Data set contains only fully recorded reflections. [d] Data set contains fully and combined partially recorded reflections. Figures in brackets represent values for the highest-resolution shell: 2.56−2.50 Å for crystal 1 and 2.05−2.00 Å for crystal 2.

PS390 graphics system using the program FRODO (Jones, 1978). The native model for active enzyme (Parsons *et al*., 1995), which contains an Ala residue at the TPQ site, was used for phases and calculated structure factors and as the starting model for the 2-HP complex with active ECAO collected at 277 K. A model for the derivatized cofactor was built by combining a planar TPQ model with the coordinates of the 2-HP moiety from the crystal structure of bis(2-hydrazinopyridine-*N*,*N*′)copper(I) iodide (Healy *et al*., 1988), using standard geometry to link the moieties. The molecular model was refined by the Hendrickson−Konnert least-squares method, using PROLSQ (Collaborative Computational Project Number 4, 1994) with the subunits treated independently. The refined model for the room-temperature 2.5 Å data was used as the starting model for the 2.0 Å data collected at 100 K. Due to the lack of isomorphism between the two active ECAO/2-HP data sets, rigid body refinement was performed in XPLOR (Brünger, 1993) before commencing atomic positional and temperature factor refinement in PROLSQ.

Gene Cloning. Plasmid pEC1 carrying the *E. coli* copper amine oxidase gene (Parsons *et al*., 1995) was digested with *Bam*HI and *Pst*I and fractionated through a 1% agarose gel. The gel slice containing the 2.2 kb ECAO gene fragment was purified using the GeneClean system (BIO101). The expression plasmid pALTER-*Ex*2 (Promega) was similarly digested, dephosphorylated with calf intestinal alkaline phosphatase (Promega), and gel fractionated, and the 5.8 kb vector was GeneClean purified. These fragments were ligated, transformed into *E. coli* JM109, and screened by alkaline lysis minipreps (Sambrook *et al*., 1989). A clone, pEAO1, that gave the expected *Hin*dIII restriction pattern was subjected to DNA sequencing using available primers (Parsons *et al*., 1995) with data collection and analysis on an ABI373A instrument (Perkin-Elmer).

pEAO1 was modified to incorporate a hexahistidine (6-His) tag to facilitate rapid purification of the protein. A cassette was constructed from the two oligonucleotides:

5′-*TATG*CATCATCATCATCATCAT**ATCGAAGGTCGC***CA*-3′ and

5′-*TATG***GCGACCTTCGAT**ATGATGATGATGATG*CA*-3′.

The *Nde*I compatible ends are in italics, and a new *Nsi*I site is underscored. The region encoding the 6-His sequence is in a larger font, and a factor Xa cleavage site coding region is in bold. These oligonucleotides were phosphorylated and annealed according to the protocols of Richards (1991) and were then ligated with *Nde*I-digested and dephosphorylated pEAO1. Following transformation of *E. coli* JM109, plasmid DNA minipreps were screened for the presence of an *Nsi*I site introduced as part of the cassette. The resulting plasmid, pEAO2, was subjected to sequence analysis as before.

Mutagenesis. pEAO1 was used as a template in the Altered Sites II (Promega) mutagenesis protocol. The system relies upon oligonucleotide primer-directed repair of a 4 bp deletion in the chloramphenicol resistance gene and introduction of a 4 bp deletion in the tetracycline resistance gene. The result is a switch of the antibiotic resistance profile of the plasmid from Cm^S/Tet^R to Cm^R/Tet^S following a successful round of mutagenesis. The mutagenic oligonucleotide 5′-CAAAAATGTAGTCA**A**AGTTACCCACTG-3′ introduced the coding change Y466F, and 5′-AGTCACCAGA**C**T**A**CAGATACGCTTTAAAG-3′ introduced the coding change D383 to an amber (TAG) termination codon. The bases changed are underscored. The procedures provided by the manufacturer were followed and proved most efficient with the alternative protocol for transfer of the mutant plasmid from the *mutS* ES1301 to JM109. This alternative protocol is based on overnight growth of the initial transformant cells rather than co-infection with a helper phage. To ensure high-efficiency transformation during the initial selection phase, electroporation rather than standard transformation was used. Briefly, 100 μL of electrocompetent *E. coli* ES1301 *mutS* cells, prepared according to the method of Sambrook *et al*. (1989), were incubated in an ice cold cuvette with 15 μL of the mutagenic synthesis reaction mixture. Following thorough mixing, the cells were subjected to an electrical discharge (400 Ω, 25 μF, 1.25 kV) in a BioRad GenePulser. The cells were diluted immediately with 1 mL of SOC medium (Sambrook *et al*., 1989) and were then added to a falcon tube containing 1 mL of 2TY medium. After a 30 min recovery period in an orbital incubator (200 rpm) at 37 °C, a further 10 mL of 2TY containing 20 μg/mL chloramphenicol was added and the culture allowed to incubate overnight to select for cells containing plasmids carrying the mutations. The remaining steps of the alternative procedure for transfer to JM109 were then followed as described in the manufacturer's protocol.

Expression and Purification of 6-His-Tagged ECAO Proteins. Mutational variant proteins, at position Asp383, were generated using the Interchange suppressor tRNA system (Promega) that comprises 13 *E. coli* strains. Twelve contain suppressor tRNAs that recognize an amber codon and introduce an amino acid rather than terminate protein translation. A nonsuppressor strain that does not contain a suppressor tRNA and therefore results in termination of translation at the amber codon is used as a control.

The amber mutant plasmid pEAO2-D383*, where * denotes an amber (TAG) codon, was generated by substituting the *Aat*II/*Pst*I restriction fragment in pEAO2 with the corresponding fragment from pEAO1-D383*. This places

the D383* mutation within the 6-His-tagged form of ECAO, thereby facilitating rapid purification. pEAO2-D383* was transformed into the 13 strains comprising the Interchange system for protein expression and purification.

Proteins were purified either by the procedure described by Parsons *et al*. (1995) or by the following procedure that utilizes the 6-His tag. Cultures of *E. coli* cells containing pEAO2-derived plasmids were grown in 2TY medium containing appropriate antibiotics for 16 h at 37 °C. These cultures were used to inoculate (1:50 dilution) fresh prewarmed medium containing 50 mM $CuSO_4$. The new cultures were grown at 37 °C with vigorous shaking for around 2 h until they were in mid log phase ($OD_{600} = 0.7$). Expression of *ecao* was then induced by addition of IPTG to a final concentration of 2 mM followed by a further period of growth of 4−4.5 h. Cells were harvested in a prechilled centrifuge at 7000 rpm (GSA) for 10 min. All subsequent manipulations were performed at 0 °C.

The periplasm fraction, containing copper amine oxidase protein, was prepared essentially according to Cooper *et al*. (1992). The proteinase inhibitors *N*-tosyl-L-phenylalanine chloromethyl ketone (TPCK) and phenylmethanesulfonyl fluoride (PMSF) were then added to final concentrations of 43 and 870 μg mL^{-1}, respectively. Ni^{2+}-NTA resin (Qiagen) was added to the periplasm preparation at 1 mL of resin per liter of original culture volume, and the suspension was gently mixed on a rocking table for 1 h at 4 °C. The nickel-bound protein was then pelleted by centrifugation at 3000 rpm (Denley BR 401 Refrigerated Centrifuge) for 30 s. The supernatant was removed, and the resin was washed three times with gentle agitation in 15 mL of 40 mM imidazole, 300 mM NaCl, and 50 mM sodium phosphate at pH 7.8 per milliliter of resin. Bound proteins were eluted by washing the resin two times in 250 mM imidazole, 300 mM NaCl, and 50 mM sodium phosphate at pH 6 for 1 h. Eluted proteins were then dialyzed overnight against 20 mM sodium phosphate at pH 7.0. Where necessary, protein solutions were concentrated in a refrigerated spin-vac (Uniscience Ltd. Refrigerated Spin Vac).

Analysis of Variant Proteins. The purity and concentration of proteins were assessed by SDS−PAGE with Coomassie G-250 staining and by measuring absorbance at 280 nm, respectively. The presence of TPQ was determined by titration with *p*-nitrophenylhydrazine essentially according to the procedures of Janes *et al*. (1992) and Palcic and Janes (1995). Briefly, 0.1−0.3 mg of wild-type or variant ECAO in 1 mL of 100 mM sodium phosphate buffer at pH 7.2 was treated by additions of 1 μL aliquots of 1 mM *p*-nitrophenylhydrazine hydrochloride. The absorbance change at 457 nm was monitored using a Shimadzu UVPC 2401-PC spectrophotometer, and further additions were made until the absorbance showed no further increase or until addition of 2 equiv. At this point, a further 1 μL aliquot of 1 mM *p*-nitrophenylhydrazine hydrochloride was added and incubation was continued for 15 min for wild type and between 15 min and 4 h for ECAO variants. The excess *p*-nitrophenylhydrazine was removed by passage through a Bio-Rad DG 10 column. The protein peak was then divided into two equal samples; to one was added a 500 μL aliquot of 100 mM sodium phosphate at pH 7.2 and to the other a 500 μL aliquot of 4 M potassium hydroxide. The absorbance spectra of these samples were recorded.

Enzyme activity measurements were made using the coupled assay system (Parsons *et al*., 1995) with phenylethylamine as substrate at 2.5 mM. Initial rates of reaction were measured.

Activity vs pH Studies of Native E. coli Amine Oxidase. Apparent K_m and V_{max} determinations, using phenylethylamine as substrate and under saturating conditions, were made at 25 °C, over the pH range of 5.25−7.0 in 0.2 M sodium citrate buffer and over the range of 7.0−8.0 in 0.2 M sodium phosphate buffer. There was good agreement between the K_m and V_{max} determinations at pH 7.0 in the two buffers. The assay procedure for activity is described in Parsons *et al*. (1995). The data were analyzed using a nonlinear regression analysis program (Herries, 1984).

Benzylamine Oxidation by E. coli Amine Oxidase. Incubations were conducted in a coupled system containing 10.0 μmol of (*R*)- or (*S*)-[*methylene*-^{2}H]benzylamine hydrochloride [available from previous studies (Scaman & Palcic, 1992; Alton *et al*., 1995)], 13.1 μmol of NADH (Sigma), 1.3 units of ADH (horse liver alcohol dehydrogenase, Sigma), and 37 000 units of catalase (Sigma) in a total volume of 1 mL with 100 mM sodium phosphate buffer at pH 6.8 ECAO (5 units, direct assay method; Parrott *et al*., 1987) was added to each incubation tube to initiate the reaction (Alton *et al*., 1995). The relative rate of benzylamine oxidation was approximately 1% of the rate of phenylethylamine oxidation (G. Alton, and M. M. Palcic, unpublished results). After a 48 h incubation at 25 °C, the reaction mixtures were diluted to 10 mL with saturated NaCl and loaded onto reverse-phase C18 Sep-Pak cartridges (Waters). Each cartridge was rinsed with 5 mL of saturated NaCl, followed by 5 mL of ^2H_2O, and then the benzyl alcohol product was eluted directly into 5 mm NMR tubes with 0.7 mL of C^2HCl_3 (deuterated NMR solvents used in the study were obtained from Cambridge Isotope Laboratories).

Tyramine Oxidation by E. coli Amine Oxidase. For analysis of C1 stereochemistry, incubations were conducted in a coupled system containing 10.5 μmol of [1(*R*)- or [1(*S*)-^{2}H]tyramine hydrochloride [available from previous studies (Scaman & Palcic, 1992; Alton *et al*., 1995)], 13.1 μmol of NADH, 4.0 units of ADH, and 37 000 units of catalase in a total volume of 1 mL with 100 mM sodium phosphate buffer at pH 6.8 (Battersby *et al*., 1979; Coleman *et al*., 1991). ECAO (0.2 unit, direct assay method) was added to each incubation tube to initiate the reaction. The relative rate of tyramine oxidation was approximately equivalent to the rate of phenylethylamine oxidation (G. Alton and M. M. Palcic, unpublished results). After a 48 h incubation at 25 °C, the reaction mixtures were diluted to 10 mL with saturated NaCl and the *p*-hydroxyphenylethyl alcohols extracted into 10 mL of ethyl acetate. The organic layer was taken to dryness, and the resulting material was dissolved in 0.7 mL of 4:1 $(^2H_3C)_2CO/^2H_2O$ prior to ^{1}H NMR spectroscopy.

For C2 stereochemical analysis, incubations were conducted in a coupled system containing 0.5 unit of amine oxidase, 24.5 μmol of C2 dideuterated tryamine hydrochloride (MSD Isotopes) or tyramine hydrochloride (Sigma), 50.4 μmol of NADH, 8.0 units of ADH, and 28 000 units of catalase in a total volume of 2 mL with 100 mM sodium phosphate buffer at pH 6.8 (or deuterated sodium phosphate buffer for the incubation containing tyramine hydrochloride). The *p*-hydroxyphenylethyl alcohol extraction conditions are as described for the C1 stereochemical analysis.

Table 2: Model Statistics

crystal	ratio of 2-HP:ECAO subunit/ soak time	*R*-factor[a] (%)	protein residues in model[b]	no. of waters	rms deviation in bond lengths/bond angles (Å)
active ECAO	1:1/1 day	14.2 (10−2.5 Å)	7A−724A 7B−725B	827	0.016/0.034
active ECAO	5:1/30 days	20.6 (10−2.0 Å)	7A−724A 6B−725B	1064	0.010/0.035

[a] $R\text{-factor} = \sum_h |F_o(h) - F_c(h)| / \sum_h F_o(h)$. [b] All models contain a copper ion and two bound cations per subunit.

^1H and ^2H NMR Spectroscopy. ^{1}H NMR spectra were recorded at 500 MHz on a Varian Unity 500 instrument at 30 °C (benzyl alcohols) or 22 °C (*p*-hydroxyphenylethyl alcohols) as described in Alton *et al.* (1995). Benzyl alcohols were dissolved in 0.7 mL of C^2HCl_3, and *p*-hydroxyphenylethyl alcohols were dissolved in 0.7 mL of 4:1 $(^2H_3C)_2CO/^2H_2O$.

RESULTS

Complex between ECAO and 2-HP for the Data Set to 2.5 Å. A $F_{o(complex)} - F_{o(native)}$ difference map and a $2F_o - F_c$ electron density map clearly revealed the 2-HP binding in the active site of both subunits. Although the complex was the dominant form, the native structure was still evident in the maps, particularly in the B-subunit, indicating that not all the ECAO molecules within the crystal had reacted with 2-HP. This is consistent with the half-of-the-sites reactivity work of De Biase *et al*. (1996) on bovine serum amine oxidase, which shows that one of the TPQ sites reacts quickly with hydrazine-derived inhibitors, whereas the second site reacts more slowly with a 10−35% occupancy after 24 h. A summary of the final model is given in Table 2.

Complex between ECAO and 2-HP for the Data Set to 2.0 Å. To try to increase the number of ECAO subunits within the crystal complexed with 2-HP, a crystal was soaked for 30 days at a 5:1 ratio of 2-HP to ECAO subunits. Flash-freezing of the crystals enabled a data set to be collected from a single crystal, with minimal decay of the diffraction pattern during the data collection. These data at higher 2-HP concentrations and longer soak times address the question of whether the binding of 2-HP to the TPQ can be driven to completion in both subunits.

Using the model of the inhibitor complex refined against the room-temperature 2.5 Å data, rigid body refinement reduced the *R*-factor from 46 to 27% (all data from 10 to 4 Å). For atomic positional and temperature factor refinement, the van der Waals radius of the copper was set to 0.0 Å, to enable unrestrained refinement of the metal to ligand distances. The final *R*-factor for the model was 20.6% for all data from 10 to 2.0 Å. A summary of the final model is given in Table 2. The occupancy of the bound inhibitor was high in both independent subunits, as shown by the temperature factors through the TPQ/2-HP moiety, and the lack of native model features, which were evident in the 2.5 Å room-temperature data. This shows that all TPQ cofactors are reactive in ECAO, and the binding of hydrazine-derived inhibitors to this enzyme can be driven to completion. This also suggests that the disorder observed at the TPQ site in the native structure (Parsons *et al*., 1995) is not due to incomplete TPQ formation but rather to structurally distinct TPQ populations which either are all capable of reacting with 2-HP or can interconvert to the structurally reactive form.

To investigate whether the ammonium sulfate-inactivated crystals of ECAO could react with 2-HP, a 2.2 Å room-temperature data set was collected for a 50:1 soak of 2-HP to ECAO subunit over 24 h (data not shown). The difference maps revealed no binding at the active site, but a low occupancy site was seen on the surface involving residues Asp329, His324, and Lys353, close to a crystal contact.

Differences in the Active Site Electron Density of the Two Independent Subunits in the Crystallographic Asymmetric Unit. The electron densities for certain equivalent residues within the active sites of the two crystallographically distinct subunits were significantly different. The B-subunit density was well ordered throughout the active site. However, in subunit A, residues Met699 and Tyr468 and the copper ligand His524 were disordered, although two conformations were discernible for Tyr468. The positions of these residues in subunit B are shown in Figure 4a. Some of the water structure around the copper was also disordered. Due to the uncertainty about the position of some residues in the active site of subunit A, discussion of the main features of the complex will deal only with the active site model for subunit B.

Interactions between the Inhibitor, 2-HP, and the Enzyme. Upon binding of the inhibitor, the ring of the TPQ moiety, which is indistinct in the native structure (Parsons *et al*., 1995), has adopted a single conformation and orientation within the ECAO active site (Figure 5). The 2-HP has covalently reacted with the 5 position of the TPQ to form a Schiff base analog; the pyridine and quinone rings are not coplanar, suggesting a substrate Schiff base rather than a product Schiff base structure (Hartmann *et al*., 1993). The quinone ring is planar, and the O2 position is hydrogen bonded to two waters, one of which is the apical water of the copper at a distance of 2.8 Å. The head group of the conserved Asn465 spans the quinone ring, in van der Waals contact with the 3 and 5 positions (Figure 4a). The role of this residue is not clear at present. TPQ O4 is interacting with the hydroxyl of the conserved Tyr369. In this case, the density clearly indicates a short hydrogen bond between the two oxygens (Figure 4b). This is consistent with a hydrogen bond in which one of the oxygens is ionized and a proton is shared between the two electronegative atoms (Speakman, 1975), although actual proton positions cannot be observed in X-ray electron density maps at this resolution. Small molecule crystal structures, such as potassium hydrogen bis(trifluoroacetate) (Golic & Speakman, 1965), which contain a short oxygen to oxygen hydrogen bond, have a bond distance of just less than 2.45 Å. A special distance restraint was specified between the two oxygens of 2.45 Å, but the weight was reduced by a factor of 4×10^4 compared to the usual hydrogen bond distance restraint. The reduced weighting almost totally removed the restraint on the distance, and it refined to a final value of 2.3 Å. This short distance is again consistent with the proposed substrate, rather than product, Schiff base structure in the mechanism, in which O4 is ionized (Mure & Klinman, 1993). Short hydrogen bonds (or low-barrier hydrogen bonds) have been reported to play a role in catalysis and stabilization in the active sites of several other enzymes [serine proteases (Frey *et al*., 1994), citrate synthase (Usher *et al*., 1994), cytidine deaminase (Xiang *et al*., 1995), and 2-amino-3-ketobutyrate-

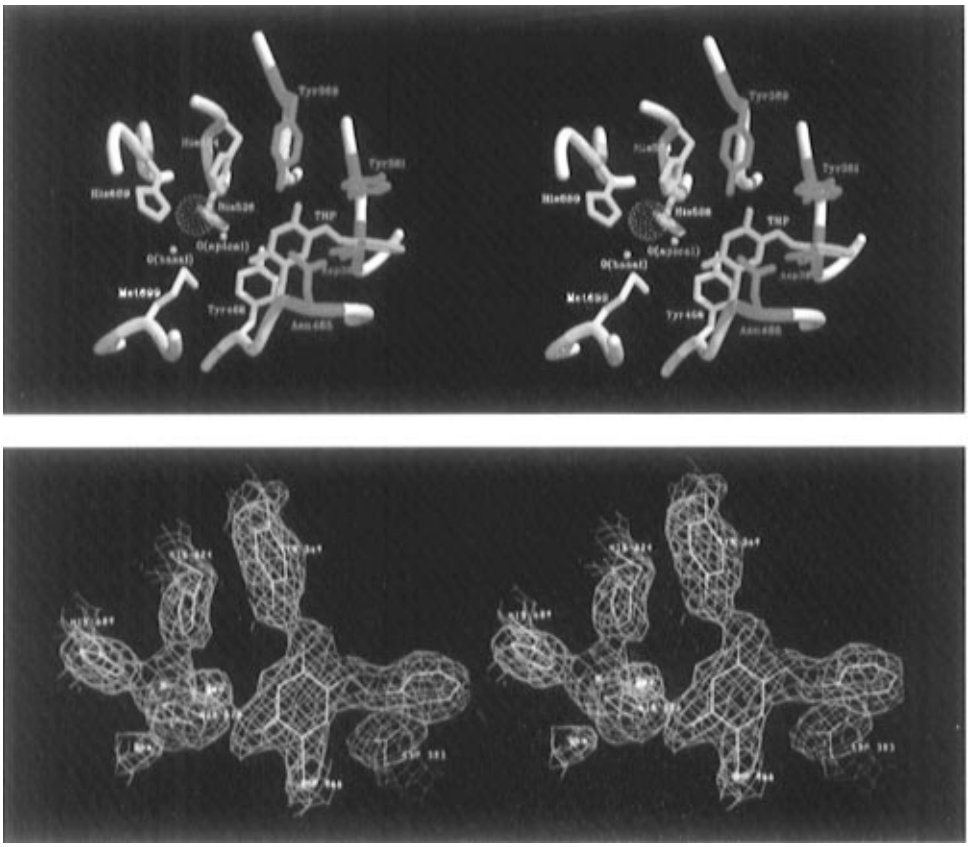

FIGURE 4: (a, top) Stereodiagram of the active site of subunit B. Only side chains referred to in the text are shown. The copper ion is represented by a green van der Waals surface. The color scheme is as follows: TPQ/inhibitor moiety (THP), green; copper ligands, blue; the base, Asp383, red; residues interacting with THP, magenta; and non-copper ligand residues which show disorder in subunit A, yellow [figure generated with MIDASPLUS (Ferrin *et al*., 1988)]. (b, bottom) Interactions with the TPQ/inhibitor moiety. Stereodiagram of a section through the final $2F_o - F_c$ map, contoured at 1.0 rms, around the site of the quinone/2-hydrazinopyridine complex (THP) and copper ion of subunit B. Only the atomic positions for the THP, the base, Asp383, Tyr369 which is involved in a short hydrogen bond with THP, and the copper ion and its ligands are shown. Only the electron density associated with the displayed atoms is shown. The basal water ligand of the copper is labeled Oba, and the apical water ligand is labeled Oax [figure generated using FRODO (Jones, 1978)].

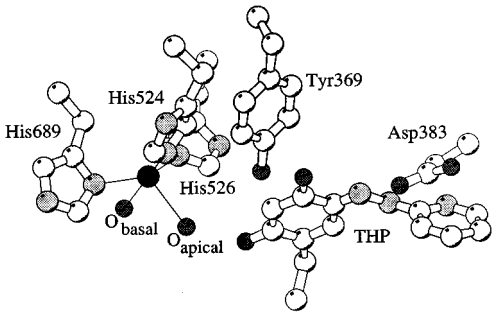

FIGURE 5: Ball-and-stick representation showing the relationship between the copper site and the TPQ/inhibitor moiety (labeled THP) in subunit B. The distorted square pyramidal coordination of the copper ligands is shown, along with the position of the base, Asp383, and the conserved Tyr369 [figure generated using MOLSCRIPT (Kraulis, 1991)].

CoA ligase (Tong & Davis, 1995)]. In ECAO, the conserved Tyr369 appears to play an important role in the stabilization and positioning of the O4 quinone anion.

The terminal hydrazine nitrogen N1 of 2-HP is covalently bonded to the C5 of the quinone ring, replacing O5 of the original TPQ. The two hydrazine nitrogens are coplanar with the quinone ring. N2 of the bound inhibitor is hydrogen bonded to the carboxylate group of Asp383 (Figure 4b). The position of N2 corresponds to C1 in the substrate, from which a proton is abstracted during the catalyzed reaction, implicating Asp383 as the general catalytic base. The pyridine ring nitrogen is hydrogen bonded to the other Asp383 carboxylate oxygen, suggesting either that this nitrogen is protonated or that Asp383 is still protonated. When compared to the native model (data to 2.4 Å, Parsons *et al*., 1995), Asp383 appears to shift slightly to optimize these two hydrogen bonds. Most natural substrates would not contain a group which would enable the formation of a second hydrogen bond to Asp383, and this may be a factor in preventing formation of the product Schiff base. This is consistent with the report (Buffoni, 1966) that 2-(aminoethyl)pyridine is an inhibitor of pig kidney diamine oxidase rather than a substrate.

Structure of the Copper Ion and Its Ligands. The copper and its ligands have the same overall structure in the 2-HP complex as in the native enzyme, except for the position of the basal water. The distance between the copper and the basal water is 2.0 Å in the native structure and 3.0 Å in the inhibitor complex. In the 2.5 Å room-temperature data, where the inhibitor is not fully bound, the basal water at 2.0 Å is evident as a "bulge" on the copper. In the 2.0 Å maps, where the inhibitor concentration is higher, the bulge is lost, and the water peak is fully resolved from the copper. Although the quinone/2-HP moiety is only indirectly linked to the copper via a hydrogen bond between the TPQ O2 and the apical water, the lengthening of the basal water to copper distance demonstrates that the copper is sensitive to the state of the quinone group. In the 2-HP complex, the basal water makes no direct interactions with the protein but is part of a hydrogen-bonded water network, which does not involve the apical water.

Site-Directed Mutagenesis of the Candidate for the Catalytic Base, Asp383. To examine the importance of Asp383, implicated in the inhibitor complex as the general base in the catalytic mechanism, we substituted this residue for a number of other amino acids. This was achieved by a combination of site-directed mutagenesis with the Altered-Sites II system and the Interchange systems (Promega). In this approach, a single directed mutant gene was generated, in which the Asp383 codon was altered to an amber UAG translation termination codon. Introducing this mutant gene (Asp383*) into a series of *E. coli* strains harboring different suppressor tRNAs allowed the production of 12 variant proteins each containing a different amino acid in place of Asp383. In early experiments, it was clear that suppressor strain efficiency varied. Some strains produced large amounts of protein, while others produced very little. Although some of the suppressor genes are chomosomal and others are carried on a ColE1-derived plasmid, there was no correlation between suppressor efficiency and copy number of the suppressor tRNA gene. To overcome the problem of purifying differential amounts of protein from equivalent culture volumes, we opted for a rapid affinity purification system. A hexahistidine-encoding (6-His) cassette was introduced to an *Nde*I site, between the codons for residues 6 and 7 of domain D1 of the mature ECAO. Although the function of this N-terminal domain is unclear, it is not found in all amine oxidases, indicating that it is not critical for enzyme activity. This suggests that the 6-His addition should not adversely affect the protein. A factor Xa cleavage site was included in the cassette to allow removal of the 6-His tag as required. Purification of 6-His/ECAO protein was rapidly achieved by Ni^{2+}-NTA affinity chromatography for 12 variants (G, P, Y, E, Q, L, C, K, R, H, F, and S). Proteins were also purified according to the previously reported purification procedure which involves FPLC separation (Parsons *et al*., 1995). As expected, no full-length protein was isolated from the nonsuppressor host. The addition of a 6-His sequence resulted in no change in the specific activity of the wild-type enzyme. Wild-type protein and Tyr466Phe were similarly expressed and purified to provide positive and negative controls, respectively. Residue 466 is the tyrosine that is converted to the quinone cofactor, TPQ. It has been shown for the *Arthrobacter globiformis* enzyme that substitution of this residue with phenylalanine leads to protein that is both inactive and negative in redox cycle staining, demonstrating the mutant protein's inability to form TPQ (Tanizawa *et al*., 1994). We used this mutant as a negative control in all our assays. Equivalent aliquots of the purified proteins were subjected to a preliminary analysis by gel fractionation and activity staining (data not shown). Only the wild-type ECAO showed detectable activity in this gel assay system.

The critical issue was to determine whether Asp383 is essential for TPQ formation, and this can most definitively be determined by recording absorbance scans of the proteins following reaction with *p*-nitrophenylhydrazine in neutral and alkaline pH. Figure 6 shows analysis of wild-type ECAO and the D383G and Y466F variants. Both wild type and D383G show the expected profiles indicative of the presence of TPQ. By contrast, the Y466F variant shows no absorbance in this region as expected for a protein that is unable to form TPQ. The D383G profile is typical of most of the variants analyzed.

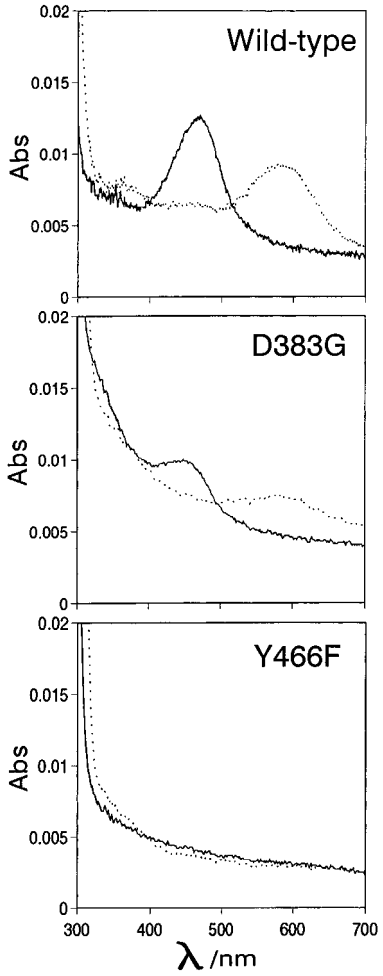

FIGURE 6: Spectrophotometric analysis of wild-type, D383G, and Y446F forms of ECAO following reaction with *p*-nitrophenylhydrazine: (—) 100 mM sodium phosphate at pH 7.2 and (•••) 2 M potassium hydroxide.

The specific activity of the wild-type ECAO was 12.76 μmol mg^{-1} min^{-1} which is in the normal range for this enzyme. By contrast, the D383G and Y466F showed no measurable activities. Similarly, other variants examined have shown no measurable activity with the exception of D383E which shows a very low but measurable activity of 5.13×10^{-5} μmol mg^{-1} min^{-1}. If any of the other variants retain some activity, then it must be at a level well below the (2.5×10^5)-fold reduced activity detectable in D383E.

These results show that Asp383 is not essential for quinone formation, consistent with the mechanisms proposed by Tanizawa (1995) and Cai and Klinman (1994). That this residue is critical for activity is fully consistent with Asp383 being the catalytic base. Of particular interest is the fact that glutamic acid is only able to restore activity to a very low level. This suggests that the presence of a carboxylate group within the enzyme structure is critical for function and that its exact position is important for enzymatic activity.

Apparent K_m and V_{max} vs pH Studies for Phenylethylamine for Native E. coli Amine Oxidase. Plots of K_{cat}/K_m *vs* pH (data not shown) reveal a bell-shaped profile centered on pH 7.0, and with apparent pK_a values of 6.2 and 8.0. Similar p*K*s and more extensive data have been obtained for bovine serum amine oxidase (Farnum *et al*., 1986) and interpreted in terms of an active site base with a p*K* of 8.0 in the native enzyme, decreasing to 5.6 in the enzyme/substrate complex. The high pK_a of 8.0 is consistent with the native ECAO

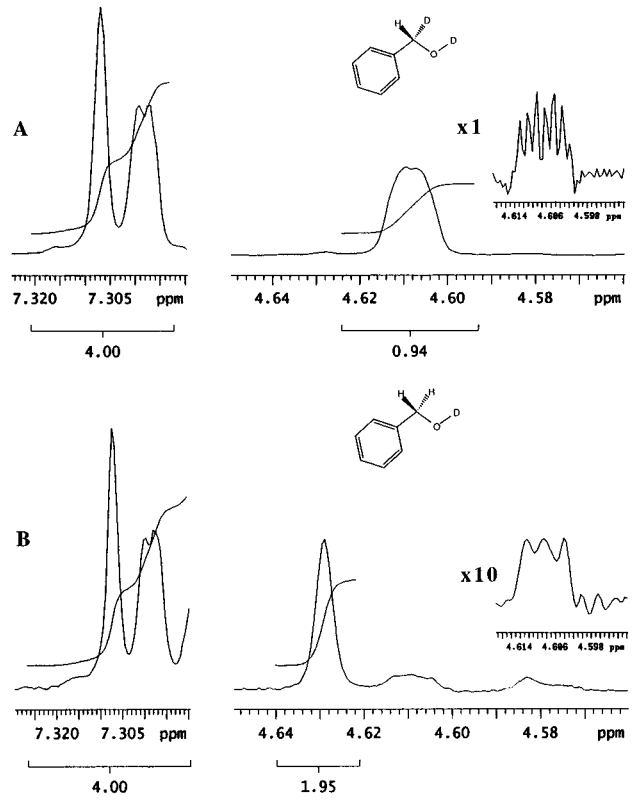

FIGURE 7: Partial 500 MHz ^{1}H NMR spectra of benzyl alcohols derived from the coupled incubations of *E. coli* amine oxidase with (*R*)-[*methylene*-^{2}H]benzylamine (A) and (*S*)-[*methylene*-^{2}H]benzylamine (B). The left-hand panels display the resonances for the aromatic protons, and the right-hand panels display the resonances for the benzylic protons. The insets are resolution-enhanced signals for the resonances observed at approximately 4.610 ppm.

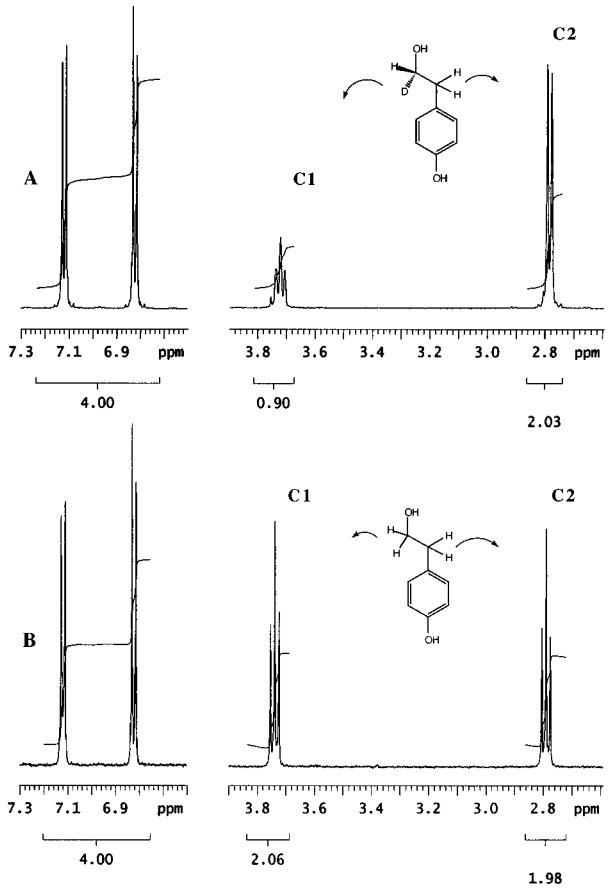

FIGURE 8: Partial 500 MHz ^{1}H NMR spectra of the *p*-hydroxyphenylethyl alcohols derived from coupled incubations of [1(*R*)-^{2}H]-tyramine (A) and [1(*S*)-^{2}H]tyramine (B) with *E. coli* amine oxidase. The left-hand panels display the aromatic proton resonances, and the right-hand panels display the C1 and C2 proton resonances.

structure (Parsons *et al*., 1995) in which Asp383 is buried in a hydrophobic environment.

Determination of the Stereospecificity of E. coli Amine Oxidase. Due to the differing stereospecificities observed for copper amine oxidases from different sources, it is important to know the stereospecific class to which ECAO belongs. We have, therefore, determined the stereospecificity of ECAO to assist in the interpretation of the structure of the complex between ECAO and the inhibitor, 2-HP.

The stereospecific retention or loss of deuterium from deuterium-labeled benzylamine or tyramine during the coupled enzymatic oxidation is conveniently followed by ^{1}H NMR spectroscopy of the isolated alcohol products. Integration (proton inventory) of the benzylic proton resonance (*vs* the aromatic protons) and determination of deuterium−proton scalar coupling provide sufficient information to follow the deuterium content of labeled amines during the course of the reaction. Prior to the stereochemical analysis of the ECAO stereochemistry, the extent of deuteration and the chiral purity of the substrate amines were validated by previously published procedures (Coleman *et al*., 1991; Scaman & Palcic, 1992).

Figure 7A shows the partial 500 MHz ^{1}H NMR of the benzyl alcohol product isolated from the incubation of (*R*)-[*methylene*-^{2}H]benzylamine with *E. coli* amine oxidase. The left panel displays the aromatic region that is identical to a commercial sample of benzyl alcohol and is assigned as four protons. Neither the resonance of the aromatic hydrogen, which is *para* relative to the benzylic carbon, nor its integration is included in this figure. A resonance at 4.607 ppm, which integrates to 0.94 proton *vs* the aromatics, is shown in the right panel of Figure 7A and is attributed to a single benzylic proton. Thus, monodeuterated benzyl alcohol was formed during the reaction, indicating that only the (*S*)-hydrogen was removed from (*R*)-[*methylene*-^{2}H]benzylamine.

Figure 7B displays the ^{1}H NMR spectra of the benzyl alcohol is isolated from the ADH-coupled incubation of (*S*)-[*methylene*-^{2}H]benzylamine with *E. coli* amine oxidase. The right panel of Figure 7B shows a resonance at 4.628 ppm that integrates to 1.95 protons *vs* the aromatic region and is thus attributed to two benzylic protons. Thus, diprotonated benzyl alcohol was formed during the enzymatic reaction. Therefore, it can be concluded that ECAO removes deuterium from *S*-deuterated benzylamine and hydrogen from *R*-deuterated benzylamine, consistent with stereospecific *pro-S* proton abstraction.

In contrast to the uniform stereochemistry of benzylamine oxidation (*pro-S*), the copper amine oxidases display heterogeneity for C1 hydrogen abstraction from tyramine or dopamine (Mondovi, 1985; Alton *et al*., 1995). Figure 8A displays the partial 500 MHz ^{1}H NMR spectrum for the *p*-hydroxyphenylethyl alcohol isolated from the coupled incubation of ECAO with [1(*R*)-^{2}H]tyramine. The left panel shows the aromatic protons. The right panel shows the C2 protons of the product alcohol as a doublet at 2.78 ppm. The C1 protons are observed as a triplet at 3.72 ppm and integrate to 0.90 proton. Within experimental error, these results show no loss of deuterium from [1(*R*)-^{2}H]tyramine during the reaction.

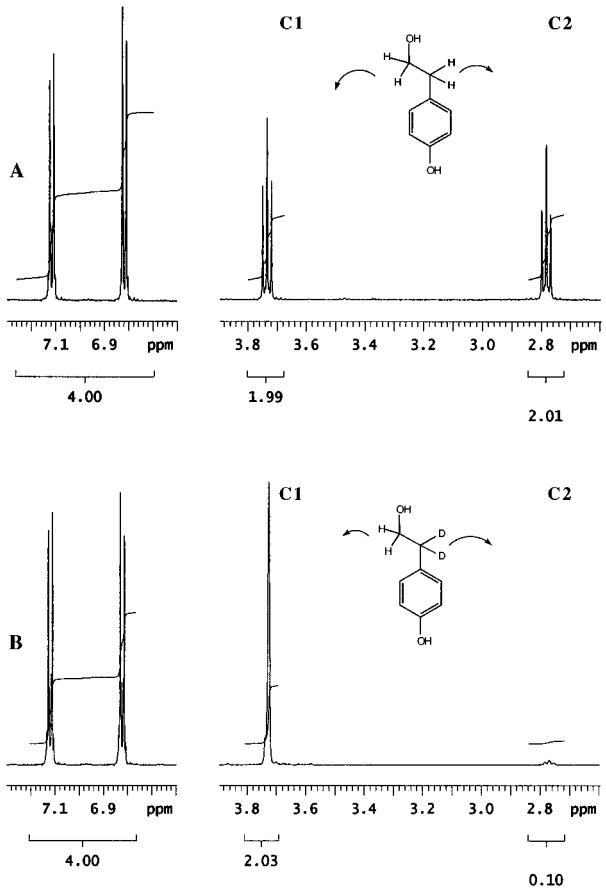

FIGURE 9: Partial 500 MHz ^{1}H NMR spectra of the *p*-hydroxyphenylethyl alcohols derived from coupled incubations of tyramine in deuterated buffer (A) and [2,2-^{2}H]tyramine in protiated buffer (B) with *E. coli* amine oxidase. The left-hand panels display the aromatic proton resonances, and the right-hand panels display the C1 and C2 proton resonances.

Figure 8B displays the spectrum of the *p*-hydroxyphenylethyl alcohol isolated from the coupled incubation of ECAO with [1(*S*)-^{2}H]tyramine. Integration of the C1 triplet at 3.74 ppm indicates 2.06 protons. Both the integration and the scalar coupling pattern indicate that the isolated *p*-hydroxyphenylethyl alcohol is fully protonated. Thus, during the enzymatic reaction of [1(*S*)-^{2}H]tyramine, the deuterium was fully removed. These results, taken together with the results of the [1(*R*)-^{2}H]tyramine incubation, indicate that the *E. coli* amine oxidase displayed only *pro-S* stereochemistry during the oxidative deamination of tyramine.

Soluble copper amine oxidase enzymes that are *pro-S* specific for hydrogen abstraction at C1 do not catalyze hydrogen exchange at C2 of the product. To investigate the loss or retention of hydrogen from C2, duplicate coupled incubations were set up. One incubation was performed in protiated buffer containing C2 dideuterated tyramine and the other in deuterated buffer with fully protonated tyramine. Figure 9A shows the partial 500 MHz ^{1}H NMR spectra for the oxidative deamination of tyramine in deuterated buffer by ECAO. The left panel shows the aromatic proton resonances, and the right panel shows the C1 and C2 proton resonances. These results indicate complete retention of hydrogen at C2 with no "wash-in" of deuterium from the deuterated buffer.

Figure 9B shows the partial 500 MHz ^{1}H NMR spectrum of the product *p*-hydroxyphenylethyl alcohol derived from dideuterated tyramine and ECAO in protiated buffer. The right panel shows a small resonance, integrating as 0.10 proton at C2. The original dideuterated tyramine contained 2% protonated tyramine as an impurity. Therefore, the small increase, from 0.04 proton equivalents to 0.10, is less than the estimated error for integration. Thus, it can be concluded that there was no significant "wash-out" of deuterium during the course of the enzymatic reaction. The *E. coli* amine oxidase does not exchange C2 hydrogens with solvent. This result conforms to the results for all other known soluble copper amine oxidases that are C1 *pro-S* specific. The *E. coli* enzyme joins a growing list of *pro-S* specific soluble copper amine oxidases that includes pea, chick pea, and soybean seedling amine oxidases and pig kidney diamine oxidase (Coleman *et al*., 1989, 1991).

DISCUSSION

Structural Changes to TPQ upon Inhibitor Binding. Although the electron density for the TPQ in the native active enzyme suggests alternative conformations, which cannot be resolved at 2.4 Å as they are too structurally similar, a "best fit" TPQ model can be modeled into the density. This model has the O4 position interacting with the hydroxyl of Tyr369, the O2 position interacting with Asp383, the candidate general base, and the O5 position closest to the copper, but not interacting with the metal ion or its ligands. Upon binding of inhibitor, a single conformation is observed, which would require a 150° ring rotation of the TPQ about its Cβ−Cγ bond from the best fit native model. This observed mobility of the ring is consistent with the proposed mechanism for TPQ biogenesis (Tanizawa, 1995; Cai & Klinman, 1994) which would require the ring to flip.

Asp383 as the Catalytic General Base. Although the proton on N2 of the 2-HP complex is interacting with Asp383, the crystallographic structure is consistent with the proton remaining on the nitrogen, and being an analog to the substrate Schiff base intermediate (Figure 1c). If the proton had been abstracted, the resulting inhibitor/quinol moiety would become a fully conjugated system, analogous to the product Schiff base intermediate, and the pyridine ring would be coplanar with the quinol ring. This is clearly not the case, with the pyridine ring lying at a 70° angle with respect to the quinone ring. In addition, studies with model systems indicate that the product Schiff base intermediate has a protonated O4 and an ionized O2 (Mure & Klinman, 1993) which is not consistent with the observed geometry in the 2-HP complex.

Therefore, if the 2-HP complex is an accurate representation of the substrate Schiff base structure, then Asp383, which lies off to one side of the inhibitor, would be on the *pro-S* hydrogen side of C1 in the substrate. The geometry is such that Asp383 would not interact with the *pro-R* hydrogen of the substrate. This is consistent with the observed stereospecificity of ECAO, in which the base abstracts only *pro-S* hydrogens from primary aromatic amine substrates. There is no other residue close to the N2 of the 2-HP which could act as the base.

The mutagenesis experiments indicate that Asp383 is critical for activity. The demonstration of TPQ in variants substituted at this position indicates that Asp383 is not essential for TPQ formation. The specific and intimate contact between the carboxylate group of Asp383 and inhibitor N2 (analogous to substrate C1) in the structure

explains why even the conservative substitution of a glutamic acid results in barely detectable activity. The additional length of the Glu side chain would lead to distortion of active site geometry upon substrate binding or could even sterically hinder substrate access to the TPQ. The position of Asp383 can explain the observed stereospecificity of proton abstraction during the ECAO reaction, and when coupled with the mutagenesis data, there would seem to be little doubt that Asp383 is indeed the catalytic base.

Entry of Substrate into the Active Site. In the native ECAO structure, the active site is buried with no obvious entry route for the monoamine substrate. In the 2-HP complex, the pyridine ring of 2-HP is almost completely buried and has displaced Tyr381, which forms a π/π ring-stacking interaction with the pyridine ring. This residue is not conserved among the known amine oxidase sequences (Tipping & McPherson, 1995), nor is there a correlation between this amino acid position having an aromatic side chain and the corresponding amine oxidases showing preferences for aromatic amine substrates. Therefore, it appears that this ring−ring interaction is not essential for aromatic substrate binding within the amine oxidase family. In fact, the range of substrates differs dramatically in the position of the aromatic portions of their structure compared to the reactive nitrogen. This suggests that the amino acids in the vicinity of the aromatic portion of the substrate (whose ring orientation will change during the reaction as the substrate C1 changes from tetrahedral to trigonal) must be able to reorganize around a variety of aromatic ring positions. Therefore, it would appear that interactions with the aromatic parts of the substrate are not very specific. It will be interesting to see how the structures of some of the other known inhibitors, which mimic different substrates, are accommodated in the active site.

The tip of the pyridine ring is at the molecular surface and is located at the edge of the interface between D3 and D4. This suggests that the point of entry for substrate into the active site is from beneath the mushroom cap of the dimer. The site is not very accessible and must be dependent on movement between D3 and D4 for opening of the site. Further evidence comes from crystal packing, and the differential occupancy of the inhibitor site in the two crystallographically independent subunits of the room temperature 2.5 Å data set. The ratio of inhibitor to enzyme subunit during the soak was 1:1. Neither subunit binding site appears to be fully occupied in this case, but intriguingly fewer subunit B active sites are occupied in the crystal by the 2-HP complex than subunit A sites. This is indicated by a higher average temperature factor for the quinone/2-HP moiety of 61 Å^2 in subunit B, while in subunit A, the average temperature factor is 40 Å.^{2} This correlates with the differing crystal contacts to D3 in the two subunits. In subunit B, there is a symmetry-related molecule, which contacts D3 and D2 from the side of the cap, while in subunit A, a symmetry-related molecule in this region only interacts with D2. This probably restricts the relative movement between D3 and D4 in subunit B and gives less opportunity for the inhibitor to reach the active site.

D3 forms the back of the complex binding pocket; with larger substrate/inhibitor complexes, residues in D3 would probably form interactions with the attached substrate/inhibitor aromatic or alkyl group. The role of D3 in forming part of the binding pocket could explain the lack of activity

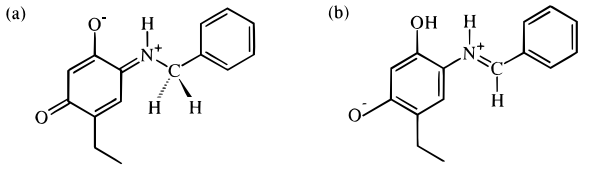

FIGURE 10: Proposed intermediates in the conversion of benzylamine to benzylaldehyde catalyzed by *E. coli* amine oxidase: (a) the substrate Schiff base intermediate and (b) the product Schiff base intermediate.

observed for a proteolytic fragment of *Hansenula polymorpha* yeast amine oxidase (Plastino & Klinman, 1995). The fragment consisted of only the D4 domain (cleaved at Glu230, which is equivalent, on the basis of sequence alignments, to Asp294 in ECAO and which is in the loop connecting D3 to D4). Although the fragment was shown to contain copper and TPQ, there was no measurable activity for methylamine and ethylamine substrates.

Stereospecificity of Copper Amine Oxidases. The inhibitor, 2-HP, is most similar in structure to the ECAO substrate, benzylamine. All copper amine oxidases so far studied abstract the *pro-S* proton from this substrate. The structural changes to a TPQ/benzylamine moiety, upon formation of the fully conjugated coplanar product Schiff base intermediate from the substrate Schiff base intermediate conformation suggested by the inhibitor complex (Figure 10), would involve reorganization of the protein. This may explain why the oxidation of benzylamine is 1% of that of phenylethylamine and tyramine, whose product Schiff base intermediates would retain torsional freedom between the substrate aromatic ring and the quinol ring, minimizing reorganization of the protein. Tyramine could be modeled in the active site positioning the *pro-S* proton close to Asp383, assuming the orientation of the TPQ moiety to be the same as in the 2-HP/ECAO complex structure. The ring of the tyramine was pointing into the solvent between domains D4 and D3. By assuming sterically preferred χ angles around the rotatable bonds within the model, the *pro-R* proton could be positioned next to Asp383. However, the tyramine ring would need to become fully buried within the protein, involving more reorganization of the protein than in the *pro-S* proton-presenting conformation. This probably explains why the *pro-S* proton is abstracted from all substrates of ECAO.

The modeling may explain the observation that there is another step, which is partially rate-limiting, in addition to the proton abstraction step for copper amine oxidases which demonstrate *pro-R* proton abstraction (Coleman *et al*., 1991). Substrate may initially bind in the more solvent-exposed *pro-S*-like conformation, which would be compatible with entry of substrate into the active site. A conformational change could then occur to the *pro-R* conformation, burying the R group attached to C2 inside the protein. The rate of this step compared to that of the proton abstraction step would then determine the stereospecific class of enzyme to which a particular amine oxidase belonged. Of the copper amine oxidases whose sequences and stereochemistry are known, only one, bovine serum amine oxidase (BSAO), does not abstract the *pro-S* proton exclusively from tyramine. This enzyme can abstract either the *pro-S* or *pro-R* proton from C1 of substrate and can exchange with solvent at C2. By examination of the sequence, it is not obvious why a *pro-R* conformation should be more favored in this enzyme than in ECAO or the other *pro-S* proton-abstracting amine

oxidases. Similar residues are observed at all the sites where steric clashes were seen in the modeling of tyramine intermediates into the 2-HP/ECAO structure.

Proton abstraction at C2 of the product imine intermediate to yield the enamine is the proposed mechanism which leads to solvent exchange (Figure 2). Modeling of the product imine intermediate into the *E. coli* amine oxidase structure suggests that Asp383 could also be involved in proton abstraction from C2, giving the enamine in amine oxidases where solvent exchange is observed (Farnum & Klinman, 1986; Palcic *et al*., 1995).

Structural Changes in Subunit A Molecules within the Crystal Soaked for 30 Days in a 2-HP to ECAO Subunit Ratio of 5:1. The disorder observed in the subunit A active site is probably significant. The inhibitor appears to be bound at an equivalent occupancy in the A- and B-subunits, as indicated by the average temperature factors of the quinone/2-HP moiety (27 $Å^2$ in A and 30 $Å^2$ in B) and the good quality of the density. The density for the ring of the copper ligand His524 suggests that, in the alternative subunit A structure, this residue is no longer coordinated to the copper. There also appears to be little or no density for a basal water, and the water structure is poorly ordered in this area. The apical water, however, is well ordered. Met699 interacts with the network of waters involved with the basal water, and its disorder is probably linked to the changes in this network. The implied loss of two of the copper ligands could indicate the reduction of the copper(II) ion to copper(I) in some of the molecules of the more accessible subunit A of the crystal during the month long soak. The proposed mechanism of the reaction, however, does not involve reduction of the copper until the product aldehyde has formed (Dooley *et al*., 1991). As the inhibitor still appears bound at high occupancy, and in a form analogous to the substrate Schiff base intermediate in both subunits, the changes observed do not appear to be consistent with those expected during the turnover of substrate. Whether the 2-HP/quinone moiety changes from the substrate Schiff base analog state to another state is uncertain, although both the carbanion and product Schiff base intermediate analogs should give structural changes which would be visible in the electron density, and no such changes are evident. If the copper is being reduced, the reason and method by which this occurs is obscure. The alternative position of Tyr468 shows that it moves from being hydrogen bonded to the Nδ of the copper ligand His526 (as observed in the B-subunit) to the head group oxygen of Asp383 interacting with the inhibitor N2. Tyr468 is not conserved between all the known sequences. It occurs in all the known bacterial and mammalian sequences but is an Asn in the legume sequences. Whether this residue has a mechanistic role requires further investigation.

Summary. The work described in this paper has enabled several questions regarding the molecular basis for catalysis in copper-containing monoamine oxidases to be answered. It has shown that ECAO belongs to the *pro-S* specific class of copper-containing amine oxidases. It has demonstrated that the site of attack by substrate-like inhibitors (e.g. 2-HP) on the TPQ cofactor is indeed the O5. The orientation of the TPQ ring when bound to the inhibitor shows that the O2 is closest to the copper and is hydrogen bonded to its apical water ligand. The importance of the conserved Tyr369 appears to be in positioning the TPQ ring via a short hydrogen bond with the O4 and is consistent with this oxygen being ionized. The position of the N2 of the 2-HP complexed to TPQ, in combination with the mutagenesis experiments, identifies Asp383 as the catalytic base. If the N2 is occupied by a carbon, as in the substrate, the Asp383 is positioned to abstract the *pro-S* hydrogen, consistent with the observed stereospecificity for ECAO. A significant lengthening of the copper to basal water distance from 2.0 to 3.0 Å in the complex is observed and demonstrates structurally that, although not directly interacting with the quinone, the copper is sensitive to changes at the cofactor site. The observation that the tip of the inhibitor pyridine ring lies at the molecular surface in a cleft between D3 and D4 suggests that substrate enters at this point.

There is still much to learn about the complex redox chemistry of this ubiquitous enzyme class. In particular, questions remain regarding the role of the copper, the stereoselectivity and substrate preference of the enzymes from different sources, and the binding of the second substrate, molecular oxygen. Future structural studies on reduced enzyme and other complexes and further detailed studies of mutational variants, such as D383E, should enable many of the remaining questions to be answered.

ACKNOWLEDGMENT

We thank Judith Klinman for helpful discussions and the staff at the Daresbury SRS, particularly Pierre Rizhkallah, for help with data collection.

REFERENCES

Alton, G., Taher, T. H., Beever, R. J., & Palcic, M. M. (1995) *Arch. Biochem. Biophys. 316*, 353−361.
Azakami, H., Yamashita, M., Roh, J. H., Suzuki, H., Kumagai, H., & Murooka, Y. (1994) *J. Ferment. Bioeng. 77*, 315−319.
Battersby, A. R., Staunton, J., & Summers, M. C. (1976) *J. Chem. Soc., Perkin Trans. 1*, 1052−1056.
Battersby, A. R., Staunton, J., Klinman, J. P., & Summers, M. C. (1979) *FEBS Lett. 99*, 297−298.
Berry, M. D., Juorio, A. V., & Paterson, I. A. (1994) *Prog. Neurobiol. 42*, 375−391.
Bradford, M. M. (1976) *Anal. Biochem. 72*, 248−254.
Brown, D. E., McGuirl, M. A., Dooley, D. M., Janes, S. M., Mu, D., & Klinman, J. P. (1991) *J. Biol. Chem. 266*, 4049−4051.
Brünger, A. T. (1993) *XPLOR, version 3.1*, Yale University Press, New Haven, CT.
Buffoni, F. (1966) *Pharmacol. Rev. 18*, 1163−1199.
Cai, D., & Klinman, J. P. (1994) *Biochemistry 33*, 7647−7652.
Coleman, A. A., Hindsgaul, O., & Palcic, M. M. (1989) *J. Biol. Chem. 264*, 19500−19505.
Coleman, A. A., Scaman, C. H., Kang, Y. J., & Palcic, M. M. (1991) *J. Biol. Chem. 266*, 6795−6800.
Collaborative Computational Project Number 4 (1994) *Acta Crystallogr. D 50*, 760−763.
Collison, D., Knowles, P. F., Mabbs, F. E., Ruis, F. X., Singh, I., Dooley, D. M., Cote, C. E., & McGuirl, M. (1989) *Biochem. J. 264*, 663−669.
Cooper, R. A., Knowles, P. F., Brown, D. E., McGuirl, M. A., & Dooley, D. M. (1992) *Biochem. J. 288*, 337−340.
De Baise, D., Agostinelli, E., De Matteis, G., Mondovi, B., & Morpurgo, L. (1996) *Eur. J. Biochem. 237*, 93−97.
Dooley, D. M., McGuirl, M. A., Brown, D. E., Turovski, R. N., McIntire, W. S., & Knowles, P. F. (1991) *Nature 349*, 262−264.
Farnum, M., & Klinman, J. P. (1986) *Biochemistry 25*, 6028−6036.
Farnum, M., Palcic, M. M., & Klinman, J. P. (1986) *Biochemistry 25*, 1898−1904.
Ferrin, T. E., Huang, C. C., Jarvis, L. E., & Langridge, R. (1988) *J. Mol. Graphics 6*, 13−27.

Frey, P. A., Whitt, S. A., & Tobin, J. B. (1994) *Science 264*, 1927−1930.
Golic, L., & Speakman, J. C. (1965) *J. Chem. Soc*., 2530−2542.
Hartmann, C., & Klinman, J. P. (1987) *J. Biol. Chem. 262*, 962−965.
Hartmann, C., & Klinman, J. P. (1990) *FEBS Lett. 261*, 441−444.
Hartmann, C., Brzovic, P., & Klinman, J. P. (1993) *Biochemistry 32*, 2234−2241.
Healy, P. C., Kildea, J. D., Skelton, B. W., & White, A. H. (1988) *Aust. J. Chem. 41*, 623−633.
Herries, D. G. (1984) *Biochem. J. 223*, 551−553.
Janes, S. M., & Klinman, J. P. (1991) *Biochemistry 30*, 4599−4605.
Janes, S. M., Palcic, M. M., Scaman, C. H., Smith, A. J., Brown, D. E., Dooley, D. M., Mure, M., & Klinman, J. P. (1992) *Biochemistry 31*, 12147−12154.
Jones, T. A. (1978) *J. Appl. Crystallogr. 11*, 268−272.
Klinman, J. P., & Mu, D. (1994) *Annu. Rev. Biochem. 63*, 299−344.
Knowles, P. F., & Dooley, D. M. (1994) in *Metal Ions in Biological Systems* (Sigel, H., & Sigel, A., Eds.) Vol. 30, pp 361−403, Marcel Dekker, New York.
Kraulis, P. J. (1991) *J. Appl. Crystallogr. 24*, 946−950.
Leslie, A. G. W. (1992) in *Joint CCP4 and ESF-EACBM Newsletter on Protein Crystallography 26*, Daresbury Laboratory, Warrington, U.K.
Lovenberg, W., & Beaven, M. A. (1971) *Biochim. Biophys. Acta 251*, 452−455.
McIntire, W. S., & Hartmann, C. (1993) in *Principles and Applications of Quinoproteins* (Davison, V. L., Ed.) pp 97−171, Marcel Dekker, New York.
Mondovi, B. (1985) *Structure and Functions of Amine Oxidases*, CRC Press, Boca Raton, FL.
Mu, D., Janes, S. M., Smith, A. J., Brown, D. E., Dooley, D. M., & Klinman, J. P. (1992) *J. Biol. Chem. 267*, 7979−7982.
Mure, M., & Klinman, J. P. (1993) *J. Am. Chem. Soc. 115*, 7117−7127.
Palcic, M. M., & Janes, S. M. (1995) *Methods Enzymol. 258*, 34−38.
Palcic, M. M., Scaman, C. H., & Alton, G. (1995) *Prog. Brain Res. 106*, 41−47.
Parrott, S., Jones, S., & Cooper, R. A. (1987) *J. Gen. Microbiol. 133*, 347−351.
Parsons, M. R., Convery, M. A., Wilmot, C. M., Yadav, K. D. S., Blakeley, V., Corner, A. S., Phillips, S. E. V., McPherson, M. J., & Knowles, P. F. (1995) *Structure 3*, 1171−1184.
Plastino, J., & Klinman, J. P. (1995) *FEBS Lett. 371*, 276−278.
Richards, J. H. (1991) in *Directed Mutagenesis: A Practical Approach* (McPherson, M. J., Ed.) pp 199−216, IRL Press, Oxford.
Roh, J. H., Suzuki, H., Azakami, H., Yamashita, M., Murooka, Y., & Kumagai, H. (1994a) *Biosci., Biotechnol., Biochem. 58* (9), 1652−1656.
Roh, J. H., Suzuki, H., Kumagai, H., Yamashita, M., Azakami, H., Murooka, Y., & Mikami, B. (1994b) *J. Mol. Biol. 238*, 635−637.
Sambrook, J., Fritsch, E. F., & Maniatis, T. (1989) in *Molecular Cloning*, 2nd ed., Cold Spring Harbor Laboratory Press, Planview, NY.
Scaman, C. H., & Palcic, M. M. (1992) *Biochemistry 31*, 6829−6841.
Speakman, C. J. (1975) in *The Hydrogen Bond and Other Intermolecular Forces*, Monographs for Teachers 27, The Chemical Society, London.
Tanizawa, K. (1995) *J. Biochem. 118*, 671−678.
Tanizawa, K., Matsuzaki, R., Shimizu, E., Yorifuji, T., & Fukui, T. (1994) *Biophys. Biochem. Res. Commun. 199*, 1096−1102.
Tipping, A. J., & McPherson, M. J. (1995) *J. Biol. Chem. 270*, 16939−16946.
Tong, H., & Davis, L. (1995) *Biochemistry 34*, 3362−3367.
Usher, K. C., Remington, J., Martin, D. P., & Drueckhammer, D. G. (1994) *Biochemistry 33*, 7753−7759.
Xiang, S., Short, S. A., Wolfenden, R., & Carter, C. W., Jr. (1995) *Biochemistry 34*, 4516−4523.

BI962205J